Engineering Fracture Mechanics Vol. 20, No. 5/6, pp. 743–766, 1984
Printed in the U.S.A.

0013–7944/84 \$3.00 + .00
Pergamon Press Ltd.

STRESS CONCENTRATION OF A CYLINDRICAL BAR WITH A V-SHAPED CIRCUMFERENTIAL GROOVE UNDER TORSION, TENSION OR BENDING

HIRONOBU NISITANI
Faculty of Engineering, Kyushu University, Fukuoka 812, Japan

and

NAO-AKI NODA
Department of Mechanical Engineering, Kyushu Institute of Technology, Tobata, Kitakyushu 804, Japan

Abstract—The stress concentration of a cylindrical bar with a V-shaped circumferential groove is analyzed by the body force method. The stress field due to a ring force in an infinite body is used to solve this problem. The solution is obtained by superposing the stress fields of ring forces in order to satisfy the given boundary conditions. The present results for semi-circular notches are in close agreement with Hasegawa's results. As a result of the systematic calculation of a 60° V-shaped notch, it is found that the stress concentration factors obtained by Neuber's trigonometric rule used currently have non-conservative errors of about 10% for a wide range of notch depths. The stress concentration factors are illustrated in charts so they can be used easily in design or research.

NOTATION

ρ	root radius of notch
t	depth of notch
ω	flank angle of notch
D	cylindrical diameter
d	diameter of minimum section
ν	Poisson's ratio
(r, θ, z)	cylindrical coordinates of a point in question
(ρ, ϕ, ζ)	cylindrical coordinates of a point where a point force acts
P_r, P_θ, P_z	magnitude of a point force
F_r, F_θ, F_z	magnitude of a ring force (force per unit length)
$\rho_r, \rho_\theta, \rho_z$	density of body force (force per unit area)
$\sigma_r^P, \sigma_\theta^P, \sigma_z^P$	stresses due to a point force
$\sigma_r^{F*}, \sigma_\theta^{F*}, \sigma_z^{F*}$; $\sigma_r^F \cos\phi^*, \sigma_\theta^F \sin\phi^*, \sigma_z^F \cos\phi^*$	stresses due to a ring force
i	number of the interval in question
j	number of the interval where the body force is applied
$\sigma_i^{\rho rj}, \sigma_i^{\rho\theta j}, \sigma_i^{\rho zj}$	influence coefficients, which mean the stress induced at the midpoint of the ith interval by the unit body force acting at the jth interval
n_1	division number for base of notch
n_2	division number for flank of notch
n_3	division number for cylindrical surface
n_t	total division number ($= n_1 + n_2 + n_3$)
$\tau_{\theta z}^\infty, \sigma_z^\infty$	nominal stress for the cylindrical diameter D
τ_{net}, σ_{net}	nominal stress for the minimum diameter d
K_t	stress concentration factor based on the net section with diameter d

1. INTRODUCTION

THE STRESS concentration problem of a cylindrical bar with a circumferential groove (Fig. 1) is mainly used in practice for the design of shafts. This problem is also important for the test specimen used in order to investigate the fatigue strength of a metal. Therefore, many researchers have tried to obtain the stress concentration factors K_t of this problem over a long period. However, most of the research on this problem has treated only a few notch sizes by experiment or calculation; thus there are few papers in which the accurate stress concentration factors are shown under various geometrical conditions necessary for design or research.

Neuber proposed the so-called 'Neuber's trigonometric formula', which gives approximate values of K_t (see Ref. [1] published in 1937 (1st edn.) and 1958 (2nd edn.)). Neuber's method makes use of the exact values of the deep hyperbolic groove (K_{th}) and the shallow elliptical notch (K_{te}) in an infinitely large cylinder and gives the approximate values of K_t for cylinders having finite diameter and finite notch depth by using the following ingenious relation

$$K_t = \frac{(K_{te} - 1)(K_{th} - 1)}{\sqrt{((K_{te} - 1)^2 + (K_{th} - 1)^2)}} + 1 \tag{1}$$

where K_{te} and K_{th} are expressed as follows.

(1) In the torsion problem

$$\left.\begin{aligned} K_{te} &= 1 + \sqrt{\left(\frac{t}{\rho}\right)} \\ K_{th} &= \frac{3\left(1 + \sqrt{\left[\frac{d}{2\rho} + 1\right]}\right)^2}{4\left(1 + 2\sqrt{\left[\frac{d}{2\rho} + 1\right]}\right)}. \end{aligned}\right\} \tag{2}$$

(2) In the tension problem

$$\left.\begin{aligned} K_{te} &= 1 + 2\sqrt{\left(\frac{t}{\rho}\right)} \\ K_{th} &= \frac{1}{N}\left\{\frac{d}{2\rho}\sqrt{\left(\frac{d}{2\rho} + 1\right)} + (0.5 + \nu)\frac{d}{2\rho} + (1 + \nu)\left(\sqrt{\left[\frac{d}{2\rho} + 1\right]} + 1\right)\right\} \\ N &= \frac{d}{2\rho} + 2\nu\sqrt{\left(\frac{d}{2\rho} + 1\right)} + 2. \end{aligned}\right\} \tag{3}$$

(3) In the bending problem

$$\left.\begin{aligned} K_{te} &= 1 + 2\sqrt{\left(\frac{t}{\rho}\right)} \\ K_{th} &= \frac{1}{N}\frac{3}{4}\left(\sqrt{\left[\frac{d}{2\rho} + 1\right]} + 1\right)\left\{3\frac{d}{2\rho} - (1 - 2\nu)\sqrt{\left(\frac{d}{2\rho} + 1\right)} + 4 + \nu\right\} \\ N &= 3\left(\frac{d}{2\rho} + 1\right) + (1 + 4\nu)\sqrt{\left(\frac{d}{2\rho} + 1\right)} + \frac{1 + \nu}{1 + \sqrt{\left(\frac{d}{2\rho} + 1\right)}}. \end{aligned}\right\} \tag{4}$$

Since it is difficult to analyze the stress concentration for an actual notch shape, Neuber's rule has been used for more than 40 years. The stress concentration charts by Peterson [2] and Nisida [3], which were made on the basis of Neuber's values, have also been used. It is supposed that the error in Neuber's values of K_t is not so large; however, the accuracy of Neuber's formula has not been discussed so much.

Rushton [4] has pointed out that Neuber's value for the notch of small radius can be seriously low using the finite-difference method (FDM) in the torsion problem. Kikukawa and Sato [5, 6] have found that one of the basic assumptions in Neuber's eqn (1), which states that the value of K_t becomes larger as the notch becomes deeper, is not correct as a result of the precise strain gauge measurement in tension and bending problems. By the recent analysis of the finite-element method (FEM) [7, 8], it has also been suggested that Neuber's rule may have a non-conservative error. Accurate stress concentration factors and accurate stress distributions are required for the quantitative estimation of fatigue notch effects.

In this paper, the stress concentration problems of a cylindrical bar with a V-shaped cir-

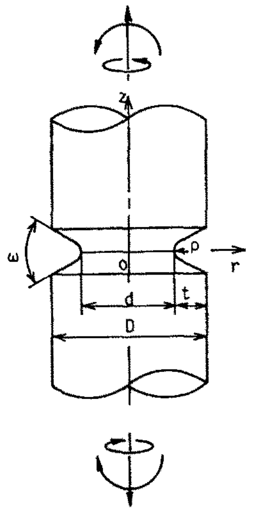

Fig. 1. A cylindrical bar with a V-shaped circumferential groove.

cumferential groove under torsion, tension or bending are analyzed by the body force method [9, 10]. The stress concentration factors K_t are systematically calculated and the accuracy of Neuber's value is discussed. Moreover, exact tables and charts of K_t necessary in design or research are shown. The present method of analysis shown below can also be used to analyze the other axisymmetric body under torsion, tension or bending.

2. METHOD OF ANALYSIS

The body force method was originally proposed by Nisitani [9] as a new method for solving the two-dimensional stress problems using a digital computer. This method was applied to various two-dimensional notch and crack problems [10, 11] in the early stages. Recently, various important three-dimensional crack problems have also been solved by this method [12–14]. The basic concept of the body force method is analogous to the boundary element method (Green's function method). However, the body force method has unique ideas in order to obtain accurate solutions; e.g. the idea of 'the basic density function of the body force' [9, 10].

In solving the two-dimensional problems, the body force method uses the stress field (Green's function) due to a point force in an infinite plate as a fundamental solution. The given boundary conditions are satisfied by applying the body force (continuously embedded point forces) along the imaginary boundaries in an infinite plate and adjusting its density so as to satisfy the specified conditions. The imaginary boundary stands for the prospective boundary for the notch or crack which should be free from stresses. In a simple problem, the density of the body force which satisfies the boundary conditions completely can be obtained in closed form. However, in a general problem, the density of the body force has to be determined by a numerical procedure. Namely, the imaginary boundaries are divided into n_t intervals and the density values are determined from the boundary conditions at the midpoint of each interval. Consequently, the method of analysis in the two-dimensional problem is summarized as follows:

(A) As the fundamental solution, the stress field due to a point force applied at a point in an infinite plate is used.

(B) The prospective boundaries are divided into finite straight or curved intervals and the given boundary conditions are satisfied at the midpoints of the intervals.

2.1 *Fundamental solutions for torsion or tension problems*

In the problems of an axisymmetric body under torsion or tension, not only the shape of the body but also the stress distribution is symmetric about the axis. Therefore, in these problems, the stress field due to continuously distributed point forces along a ring around the axis (A)* can be used as a fundamental solution instead of (A). It is easily understood that the ring forces acting in the radial and axial directions (Figs. 2(a) and (b)) give the fundamental solutions for tension problems and the ring force acting in the circumferential direction (Fig. 2(c)) gives the fundamental solution for torsion problems. The procedure (B) in a two-dimensional case

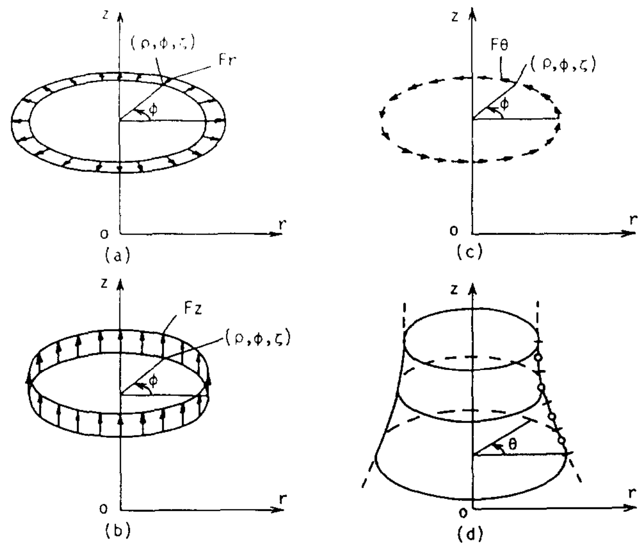

Fig. 2. Fundamental solutions for tension and torsion problems.

can be used for this case, because if the boundary conditions are satisfied at one point (the point marked ○ in Fig. 2(d)) of the circumference, the boundary conditions at all points of the circumference are satisfied naturally from axial symmetry. Therefore, the extension from two-dimensional problems to axisymmetric problems is established by changing (A), (B) into the following two terms (A)*, (B)*.

(A)* As the fundamental solution, the stress field due to point forces distributed continuously along a ring around the axis is used.

(B)* The given boundary conditions are satisfied at each representative point of the circumferences.

On the other hand, in the problem of an axisymmetric body under bending, it must be considered that the stress distribution induced by the bending moment is not axisymmetric; therefore, the analysis of bending problems is more difficult than torsion and tension problems. However, if the appropriate fundamental solutions are used, the calculation procedure becomes almost similar to that adopted previously.

2.2 *Fundamental solutions for bending problems*

Imagine an infinite body subjected to the bending moment at infinity. If we take the z-axis as the axis of symmetry and apply the bending moment around the radial axis of $\theta = \pi/2$ as shown in Figs. 3 and 4, the stresses far from the origin are expressed as

$$\sigma_z = \sigma_0 \frac{r}{a} \cos\theta, \qquad \sigma_r = \sigma_\theta = \tau_{rz} = \tau_{r\theta} = \tau_{\theta z} = 0 \tag{5}$$

where σ_0 is a constant corresponding to the magnitude of the bending stress and a is a rep-

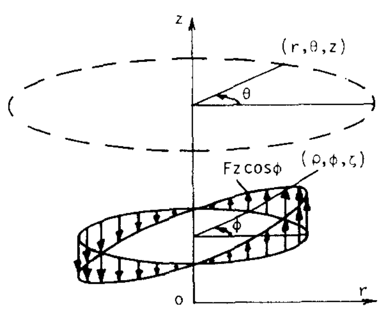

Fig. 3. A ring force with intensity cos ϕ in the z-direction.

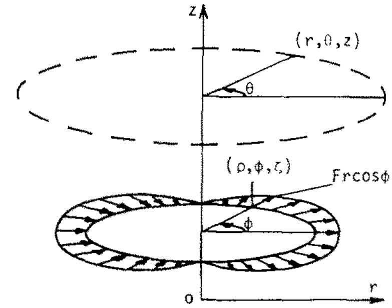

Fig. 4. A ring force with intensity cos ϕ in the r-direction.

resentative dimension. Since the stress σ_z at infinity is expressed in the form of multiples of cos θ, the stress σ_z induced by point forces distributed in the z-direction (the ring force; a fundamental solution) should also vary in the type of cos θ on the circumference of radius r and height z. Therefore, we suppose the intensities of the two ring forces in the form of multiples of cos θ; one is in the z-direction (Fig. 3) and the other is in the r-direction (Fig. 4). In these figures, (ρ, ϕ, ζ) is used as the cylindrical coordinates of a point where a point force acts. The ring force with the intensity of cos θ in the radial direction is also necessary as the fundamental solution, because the stresses in the r-direction induced by the ring force acting in the z-direction must be canceled. Thus, as will be shown in Section 3, we can find that the ring forces in both directions induce the stresses at (r, θ, z) as

$$\left.\begin{array}{lll} \sigma_r = f_1(r, \rho, z\ \zeta) \cos\theta, & \sigma_\theta = f_2(r, \rho, z, \zeta) \cos\theta, & \sigma_z = f_3(r, \rho, z, \zeta) \cos\theta \\ \tau_{rz} = f_4(r, \rho, z, \zeta) \cos\theta, & \tau_{r\theta} = f_5(r, \rho, z, \zeta) \sin\theta, & \tau_{\theta z} = f_6(r, \rho, z, \zeta) \sin\theta. \end{array}\right\} \quad (6)$$

Moreover, we can see that the normal stress σ_n and the shearing stress τ_{nt} at a point on an arbitrary curved surface imagined in the infinite body, also are expressed in the form of multiples of cos θ along the circumference

$$\left.\begin{aligned} \sigma_n &= \sigma_r \cos^2\psi_1 + \sigma_z \sin^2\psi_1 + 2\tau_{rz} \sin\psi_1 \cos\psi_1 \\ &= (f_1 \cos^2\psi_1 + f_3 \sin^2\psi_1 + 2f_4 \sin\psi_1 \cos\psi_1) \cos\theta \\ \tau_{nt} &= (-\sigma_r + \sigma_z) \sin\psi_1 \cos\psi_1 + \tau_{rz}(\cos^2\psi_1 - \sin^2\psi_1) \\ &= \{(-f_1 + f_3) \sin\psi_1 \cos\psi_1 + f_4(\cos^2\psi_1 - \sin^2\psi_1)\} \cos\theta \end{aligned}\right\} \quad (7)$$

where ψ_1 is the angle between the r-axis and the normal direction of the surface. Therefore, if the conditions $\sigma_n = \tau_{nt} = 0$ are satisfied at $r = r$ and $\theta = 0$, the same boundary conditions are automatically satisfied at all points of $\theta \neq 0$ on the same radius $r = r$. Concerning the condition σ_n and τ_{nt}, it seems that the combinations of these two kinds of ring forces applied in the z- and r-direction are sufficient for the satisfaction of the boundary conditions. However, actually the combinations of ring forces shown in Figs. 3 and 4 are insufficient, because their application induces the shearing stress $\tau_{n\theta}$ (i.e. $\tau_{r\theta}$ and $\tau_{\theta z}$) at the boundary which must become free from stresses. The shearing stress $\tau_{n\theta}$ is expressed as

$$\begin{aligned} \tau_{n\theta} &= \tau_{r\theta} \cos\psi_1 + \tau_{\theta z} \sin\psi_1 \\ &= (f_5 \cos\psi_1 + f_6 \sin\psi_1) \sin\theta. \end{aligned} \quad (8)$$

As seen from eqn (8), the shearing stress $\tau_{n\theta}$ is expressed in the form of multiples of sin θ on the radius $r = r$. Therefore, it becomes necessary to apply the tangential ring force that changes in the form of multiples of sin θ on the radius $r = \rho$ as shown in Fig. 5. The application of the ring force shown in Fig. 5 induces the stresses σ_r, σ_z, τ_{rz} that should have the form of eqn (6) again in order to satisfy the boundary conditions. As will be shown in Section 3 in detail, it is confirmed that the application of the ring forces shown in Fig. 5 fortunately induces the stress field expressed in the form of eqn (6).

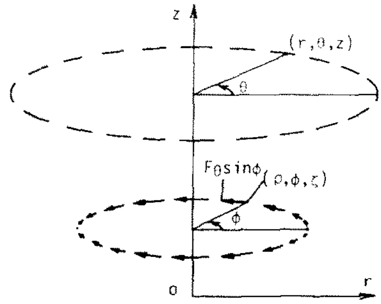

Fig. 5. A ring force with intensity sin ϕ in the θ-direction.

The above discussion leads us to the conclusion that three types of ring forces are necessary and sufficient for the satisfaction of the boundary conditions of the bending problems of an axisymmetric body [21]. In this way, the calculation procedure similar to the torsion or tension problem can be used in the bending problem of a cylindrical bar.

3. FUNDAMENTAL SOLUTIONS

When a point force P_r, P_θ, P_z acts at a point (ρ, ϕ, ζ) in an infinite body, the stresses at $(r, \theta, z$ are given by

$$\left.\begin{aligned}
\sigma_r^{P_r} &= B_r[(1-2\nu)R^{-3}[-r\cos(\varphi-\theta)+\rho\{2\cos^2(\varphi-\theta)-1\}] \\
&\quad -3R^{-5}\{r\cos(\varphi-\theta)-\rho\}\{r-\rho\cos(\varphi-\theta)\}^2] \\
\sigma_\theta^{P_r} &= B_r[(1-2\nu)R^{-3}[r\cos(\varphi-\theta)-\rho\{2\cos^2(\varphi-\theta)-1\}] \\
&\quad -3\,R^{-5}\{-r\cos(\varphi-\theta)+\rho\}\rho^2\sin^2(\varphi-\theta)] \\
\sigma_z^{P_r} &= B_r[(1-2\nu)R^{-3}-3(z-\zeta)^2R^{-5}]\{r\cos(\varphi-\theta)-\rho\} \\
\tau_{rz}^{P_r} &= B_r(z-\zeta)[-(1-2\nu)R^{-3}\cos(\varphi-\theta) \\
&\quad -3\,R^{-5}\{r\cos(\varphi-\theta)-\rho\}\{r-\rho\cos(\varphi-\theta)\{] \\
\tau_{r\theta}^{P_r} &= B_r[(1-2\nu)R^{-3}\sin(\varphi-\theta)\{2\rho\cos(\varphi-\theta)-r\} \\
&\quad +3R^{-5}\rho\sin(\varphi-\theta)\{r\cos(\varphi-\theta)-\rho\}\{r-\rho\cos(\varphi-\theta)\}] \\
\tau_{\theta z}^{P_r} &= B_r(z-\zeta)[-(1-2\nu)R^{-3}\sin(\varphi-\theta) \\
&\quad +3R^{-5}\{r\cos(\varphi-\theta)-\rho\}\rho\sin(\varphi-\theta)]
\end{aligned}\right\} \quad (9a)$$

$$\left.\begin{aligned}
\sigma_r^{P_\theta} &= B_\theta[(1-2\nu)R^{-3}\sin(\varphi-\theta)\{r-2\rho\cos(\varphi-\theta)\} \\
&\quad +3R^{-5}r\sin(\varphi-\theta)\{r-\rho\cos(\varphi-\theta)\}^2] \\
\sigma_\theta^{P_\theta} &= B_\theta[(1-2\nu)R^{-3}\sin(\varphi-\theta)\{-r+2\rho\cos(\varphi-\theta)\} \\
&\quad +3R^{-5}r\rho^2\sin^3(\varphi-\theta)] \\
\sigma_z^{P_\theta} &= B_\theta\{(1-2\nu)R^{-3}-3(z-\zeta)^2R^{-5}\}\{-r\sin(\varphi-\theta)\} \\
\tau_{rz}^{P_\theta} &= B_\theta(z-\zeta)[(1-2\nu)R^{-3}\sin(\varphi-\theta) \\
&\quad +3R^{-5}r\sin(\varphi-\theta0\{r-\rho\cos(\varphi-\theta)\}] \\
\tau_{r\theta}^{P_\theta} &= B_\theta[-(1-2\nu)R^{-3}[r\cos(\varphi-\theta)-\rho\{2\cos^2(\varphi-\theta)-1\} \\
&\quad -3\,R^{-5}r\rho\sin^2(\varphi-\theta)\{r-\rho\cos(\varphi-\theta)\}] \\
\tau_{\theta z}^{P_\theta} &= B_\theta(z-\zeta)\{-(1-2\nu)R^{-3}\cos(\varphi-\theta) \\
&\quad -3\,R^{-5}r\rho\sin^2(\varphi-\theta)\}
\end{aligned}\right\} \quad (9b)$$

$$\left.\begin{aligned}
\sigma_r^{P_z} &= B_z(z-\zeta)[(1-2\nu)R^{-3} - 3R^{-5}\{r-\rho\cos(\varphi-\theta)\}^2] \\
\sigma_\theta^{P_z} &= B_z(z-\zeta)[(1-2\nu)R^{-3} - 3R^{-5}\rho^2\sin^2(\varphi-\theta)] \\
\sigma_z^{P_z} &= B_z(z-\zeta)[-(1-2\nu)R^{-3} - 3R^{-5}(z-\zeta)^2] \\
\tau_{rz}^{P_z} &= B_z\{-(1-2\nu)R^{-3} - 3(z-\zeta)^2R^{-5}\}\{r-\rho\cos(\varphi-\theta)\} \\
\tau_{r\theta}^{P_z} &= B_z[3(z-\zeta)R^{-5}\rho\sin(\varphi-\theta)\{r-\rho\cos(\varphi-\theta)\}] \\
\tau_{\theta z}^{P_z} &= B_z\{-(1-2\nu)R^{-3} - 3(z-\zeta)^2R^{-5}\}\{-\rho\sin(\varphi-\theta)\}
\end{aligned}\right\} \quad (9c)$$

where

$$B_r = \frac{P_r}{8\pi(1-\nu)}, \quad B_\theta = \frac{P_\theta}{8\pi(1-\nu)}, \quad B_z = \frac{P_z}{8\pi(1-\nu)}$$
$$R^2 = r^2 + \rho^2 + (z-\zeta)^2 - 2r\rho\cos(\varphi-\theta).$$

In eqns (9a) and (9c), the stresses σ_r, σ_θ, σ_z, τ_{rz} due to P_r and P_{yz} are the even functions of $\phi'(=\phi-\theta)$, while the stresses $\tau_{r\theta}$, $\tau_{\theta z}$ are the odd functions of ϕ'. On the contrary, in eqn (9b), the stresses σ_r, σ_θ, σ_z, τ_{rz} due to P_θ are the odd functions of ϕ', while the stresses $\tau_{r\theta}$, $\tau_{\theta z}$ are the even functions of ϕ'. These properties of eqn (9) are important in discussing the properties of the stress fields due to ring forces shown in Figs. 2–5.

The fundamental solutions of ring forces shown in Fig. 2 are expressed as follows using eqn (9)

$$\left.\begin{aligned}
\sigma^{F_r*} &= \int_0^{2\pi} \sigma^{P_r}|_{P_r=1}\, F_r\rho\, d\varphi \\
\sigma^{F_\theta*} &= \int_0^{2\pi} \sigma^{P_\theta}|_{P_\theta=1}\, F_\theta\rho\, d\varphi \\
\sigma^{F_z*} &= \int_0^{2\pi} \sigma^{P_z}|_{P_z=1}\, F_z\rho\, d\varphi.
\end{aligned}\right\} \quad (10)$$

All of the integrands in eqn (10) are periodic functions of ϕ' (period $\neq 2\pi$). Therefore, the integrals in eqn (10) are expressed as

$$\left.\begin{aligned}
\int_0^{2\pi} f(\varphi-\theta)\, d\varphi &= \int_{-\theta}^{2\pi-\theta} f(\varphi)\, d\varphi' \\
&= \int_0^{2\pi} f(\varphi')\, d\varphi' = \int_{-\pi}^{\pi} f(\varphi')\, d\varphi' \\
&= \begin{cases} 2\int_0^{\pi} f(\varphi')\, d\varphi' & (f(\varphi')\text{: even function of } \phi') \\ 0 & (f(\varphi')\text{: odd function of } \phi'). \end{cases}
\end{aligned}\right\} \quad (11)$$

On the other hand, the fundamental solutions of ring forces shown in Figs. 3–5 are expressed as

$$\left.\begin{aligned}
\sigma^{F_r\cos\varphi*} &= \int_0^{2\pi} \sigma^{P_r}|_{P_r=1}\, F_r\rho\cos\varphi\, d\varphi \\
\sigma^{F_\theta\sin\varphi*} &= \int_0^{2\pi} \sigma^{P_\theta}|_{P_\theta=1}\, F_\theta\rho\sin\varphi\, d\varphi \\
\sigma^{F_z\cos\varphi*} &= \int_0^{2\pi} \sigma^{P_z}|_{P_z=1}\, F_z\rho\cos\varphi\, d\varphi.
\end{aligned}\right\} \quad (12)$$

The integrals in eqn (12) are expressed as in the form of eqn (13)

$$\left.\begin{aligned}
&\text{(i)}\ \int_0^{2\pi} f(\varphi-\theta)\cos\varphi\,d\varphi = \int_{-\pi}^{\pi} f(\varphi')\cos(\varphi'+\theta)\,d\varphi' \\
&= \int_{-\pi}^{\pi} f(\varphi')(\cos\varphi'\cos\theta - \sin\varphi'\sin\theta)\,d\varphi' \\
&= \begin{cases} 2\displaystyle\int_0^{\pi} f(\varphi')\cos\varphi'\,d\varphi'\cdot\cos\theta & (f(\varphi')\text{: even function of }\phi') \\ -2\displaystyle\int_0^{\pi} f(\varphi')\sin\varphi'\,d\varphi'\cdot\sin\theta & (f(\varphi')\text{: odd function of }\phi') \end{cases} \\
&\text{(ii)}\ \int_0^{2\pi} f(\varphi-\theta)\sin\varphi\,d\varphi = \int_{-\pi}^{\pi} f(\varphi')\sin(\varphi'+\theta)\,d\varphi' \\
&= \int_{-\pi}^{\pi} f(\varphi')(\sin\varphi'\cos\theta + \cos\varphi'\sin\theta)\,d\varphi' \\
&= \begin{cases} 2\displaystyle\int_0^{\pi} f(\varphi')\cos\varphi'\,d\varphi'\cdot\sin\theta & (f(\varphi')\text{: even function of }\phi') \\ 2\displaystyle\int_0^{\pi} f(\varphi')\sin\varphi'\,d\varphi'\cdot\cos\theta & (f(\varphi')\text{: odd function of }\phi'). \end{cases}
\end{aligned}\right\} \quad (13)$$

As shown in eqn. (13), it is confirmed that the stress fields of ring forces shown in Figs. 3–5 are expressed as in the form of eqn (6).

The integration with respect to ϕ' between $\phi' = 0$ and π (eqns (11) and (13) is expressed in terms of the complete elliptic integrals of the first and second kind. In the following equations, ϕ' $(= \phi - \theta)$ is replaced by a new variable ϕ.

(1) Fundamental solutions in torsion problems:

$$\left.\begin{aligned}
\tau_{r\theta}^{F_\theta *} &= \frac{F_\theta \rho}{2\pi r_m^3}(-\rho I_0 - r I_1 + 2\rho I_2) \\
\tau_{\theta z}^{F_\theta *} &= \frac{F_\theta \rho}{2\pi r_m^3}\bar{z} I_1 \\
(\sigma_r^{F_\theta *} &= \sigma_\theta^{F_\theta *} = \sigma_z^{F_\theta *} = \tau_{rz}^{F_\theta *} = 0).
\end{aligned}\right\} \quad (14)$$

(2) Fundamental solutions in tension problems:

$$\left.\begin{aligned}
\sigma_r^{F_r *} &= \frac{F_r \rho}{4\pi(1-\nu) r_m^3}[(1-2\nu)(-\rho I_0 - r I_1 + 2\rho I_2) \\
&\quad + \frac{3}{r_m^2}\{r^2\rho J_0 - r(r^2+2\rho^2)J_1 + \rho(2r^2+\rho^2)J_2 - r\rho^2 J_3\}] \\
\sigma_\theta^{F_r *} &= \frac{F_r \rho}{4\pi(1-\nu) r_m^3}[(1-2\nu)(\rho I_0 + r I_1 - 2\rho I_2) \\
&\quad + \frac{3\rho^2}{r_m^2}(\rho J_0 - r J_1 - \rho J_2 + r J_3)] \\
\sigma_z^{F_r *} &= \frac{F_r \rho}{4\pi(1-\nu) r_m^3}[(1-2\nu)(-\rho I_0 + r I_1) + \frac{3\bar{z}^2}{r_m^2}(\rho J_0 - r J_1)] \\
\tau_{rz}^{F_r *} &= \frac{F_r \rho}{4\pi(1-\nu) r_m^3}[(1-2\nu)\bar{z}(-I_1) \\
&\quad + \frac{3\bar{z}}{r_m^2}\{r\rho J_0 - (r^2+\rho^2)J_1 + r\rho J_2\}] \\
(\tau_{r\theta}^{F_r *} &= \tau_{\theta z}^{F_r *} = 0)
\end{aligned}\right\} \quad (15a)$$

$$\left.\begin{aligned}
\sigma_r^{F_z*} &= \frac{F_z\rho}{4\pi(1-\nu)r_m^3}\left[(1-2\nu)\bar{z}I_0 + \frac{3\bar{z}}{r_m^2}(-r^2J_0 + 2r\rho J_1 - \rho^2 J_2)\right] \\
\sigma_\theta^{F_z*} &= \frac{F_z\rho}{4\pi(1-\nu)r_m^3}\left[(1-2\nu)\bar{z}I_0 + \frac{3\bar{z}\rho^2}{r_m^2}(-J_0 + J_2)\right] \\
\sigma_z^{F_z*} &= \frac{F_z\rho}{4\pi(1-\nu)r_m^3}\left[(1-2\nu)\bar{z}(-I_0) + \frac{3\bar{z}^3}{r_m^2}(-J_0)\right] \\
\tau_{rz}^{F_z*} &= \frac{F_z\rho}{4\pi(1-\nu)r_m^3}\left[(1-2\nu)(-rI_0 + \rho I_1) + \frac{3\bar{z}^2}{r_m^2}(-rJ_0 + \rho J_1)\right] \\
(\tau_{r\theta}^{F_z*} &= \tau_{\theta z}^{F_z*} = 0)
\end{aligned}\right\} \tag{15b}$$

(3) Fundamental solutions in bending problems:

$$\left.\begin{aligned}
\sigma_r^{F_r\cos\varphi*} &= \frac{F_r\rho\cos\theta}{4\pi(1-\nu)r_m^3}\Big[(1-2\nu)(-\rho I_1 - rI_2 + 2\rho I_3) \\
&\quad + \frac{3}{r_m^2}\{r^2\rho J_1 - r(r^2+2\rho^2)J_2 + \rho(2r^2+\rho^2)J_3 - r\rho^2 J_4\}\Big] \\
\sigma_\theta^{F_r\cos\varphi*} &= \frac{F_r\rho\cos\theta}{4\pi(1-\nu)r_m^3}\Big[(1-2\nu)(\rho I_1 + rI_2 - 2\rho I_3) \\
&\quad + \frac{3\rho^2}{r_m^2}(\rho J_1 - rJ_2 - \rho J_3 + rJ_4)\Big] \\
\sigma_z^{F_r\cos\varphi*} &= \frac{F_r\rho\cos\theta}{4\pi(1-\nu)r_m^3}\left[(1-2\nu)(-\rho I_1 + rI_2) + \frac{3\bar{z}^2}{r_m^2}(\rho J_1 - rJ_2)\right] \\
\tau_{rz}^{F_r\cos\varphi*} &= \frac{F_r\rho\cos\theta}{4\pi(1-\nu)r_m^3}\Big[(1-2\nu)\bar{z}(-I_2) \\
&\quad + \frac{3\bar{z}}{r_m^2}\{r\rho J_1 - (r^2+\rho^2)J_2 + r\rho J_3\}\Big] \\
\tau_{r\theta}^{F_r\cos\varphi*} &= \frac{F_r\rho\sin\theta}{4\pi(1-\nu)r_m^3}\Big[(1-2\nu)(rI_0 - 2\rho I_1 - rI_2 + 2\rho I_3) \\
&\quad + \frac{3\rho}{r_m^2}\{r\rho J_0 - (r^2+\rho^2)J_1 + (r^2+\rho^2)J_3 - r\rho J_4\}\Big] \\
\tau_{\theta z}^{F_r\cos\varphi*} &= \frac{F_r\rho\sin\theta}{4\pi(1-\nu)r_m^3}\Big[(1-2\nu)\bar{z}(I_0 - I_1) \\
&\quad + \frac{3\bar{z}\rho}{r_m^2}(\rho J_0 - rJ_1 - \rho J_2 + rJ_3)\Big]
\end{aligned}\right\} \tag{16a}$$

$$\begin{aligned}
\sigma_r^{F_\theta\sin\varphi*} &= \frac{F_\theta\rho\cos\theta}{4\pi(1-\nu)r_m^3}\Big[(1-2\nu)(rI_0 - 2\rho I_1 - rI_2 + 2\rho I_3) \\
&\quad + \frac{3\rho}{r_m^2}\{r^2J_0 - 2r\rho J_1 - (r^2-\rho^2)J_2 + 2r\rho J_3 - \rho^2 J_4\}\Big] \\
\sigma_\theta^{F_\theta\sin\varphi*} &= \frac{F_\theta\rho\cos\theta}{4\pi(1-\nu)r_m^3}\Big[(1-2\nu)(-rI_0 + 2\rho I_1 + rI_2 - 2\rho I_3) \\
&\quad + \frac{3r\rho^2}{r_m^2}(J_0 - 2J_2 + 4J_4)\Big]
\end{aligned}$$

$$\left.\begin{aligned}
\sigma_z^{F_\theta \sin\varphi *} &= \frac{F_\theta \rho \cos\theta}{4\pi(1-\nu)r_m^3}\left[(1-2\nu)r(-I_0+I_2)+\frac{3r\bar{z}}{r_m^2}(J_0-J_2)\right]\\
\tau_{rz}^{F_\theta \sin\varphi *} &= \frac{F_\theta \rho \cos\theta}{4\pi(1-\nu)r_m^3}\left[(1-2\nu)\bar{z}(I_0-I_2)\right.\\
&\qquad\left.+\frac{3r\bar{z}}{r_m^2}(rJ_0-\rho J_1-rJ_2+\rho J_3)\right]\\
\tau_{r\theta}^{F_\theta \sin\varphi *} &= \frac{F_\theta \rho \sin\theta}{4\pi(1-\nu)r_m^3}\left[(1-2\nu)(-\rho I_1-rI_2+2\rho I_3)\right.\\
&\qquad\left.+\frac{3r\rho}{r_m^2}(-rJ_1+\rho J_2+rJ_3-\rho J_4)\right]\\
\tau_{\theta z}^{F_\theta \sin\varphi *} &= \frac{F_\theta \rho \sin\theta}{4\pi(1-\nu)r_m^3}\left[(1-2\nu)\bar{z}(-I_2)+\frac{3r\rho\bar{z}}{r_m^2}(-J_1+J_3)\right]
\end{aligned}\right\} \tag{16b}$$

$$\left.\begin{aligned}
\sigma_r^{F_z \cos\varphi *} &= \frac{F_z \rho \cos\theta}{4\pi(1-\nu)r_m^3}\left[(1-2\nu)\bar{z}I_1+\frac{3\bar{z}}{r_m^2}(-r^2J_1+2r\rho J_2-\rho^2 J_3)\right]\\
\sigma_\theta^{F_z \cos\varphi *} &= \frac{F_z \rho \cos\theta}{4\pi(1-\nu)r_m^3}\left[(1-2\nu)\bar{z}I_1+\frac{3\bar{z}\rho^2}{r_m^2}(-J_1+J_3)\right]\\
\sigma_z^{F_z \cos\varphi *} &= \frac{F_z \rho \cos\theta}{4\pi(1-\nu)r_m^3}\left[(1-2\nu)\bar{z}(-I_1)+\frac{3\bar{z}^3}{r_m^2}(-J_1)\right]\\
\tau_{rz}^{F_z \cos\varphi *} &= \frac{F_z \rho \cos\theta}{4\pi(1-\nu)r_m^3}\left[(1-2\nu)(-rI_1+\rho I_2)+\frac{3\bar{z}^2}{r_m^2}(-rJ_1+\rho J_2)\right]\\
\tau_{r\theta}^{F_z \cos\varphi *} &= \frac{F_z \rho \sin\theta}{4\pi(1-\nu)r_m^3}\left[+\frac{3\rho\bar{z}}{r_m^2}(-rJ_0+\rho J_1+rJ_2-\rho J_3)\right]\\
\tau_{\theta z}^{F_z \cos\varphi *} &= \frac{F_z \rho \sin\theta}{4\pi(1-\nu)r_m^3}\left[(1-2\nu)\rho(-I_0+I_2)+\frac{3\rho\bar{z}^2}{r_m^2}(-J_0+J_2)\right]
\end{aligned}\right\} \tag{16c}$$

where

$$\left.\begin{aligned}
r_m &= \sqrt{(2r\rho)}, \quad \bar{z} = z-\zeta\\
I_n &= \int_0^\pi \frac{\cos^n\varphi}{(e-\cos\varphi)^{3/2}}\,d\varphi, \quad J_n = \int_0^\pi \frac{\cos^n\varphi}{(e-\cos\varphi)^{5/2}}\,d\varphi\\
I_0 &= \frac{1}{e^2-1}K_1\\
I_1 &= \frac{e}{e^2-1}K_1 - K_2\\
I_2 &= \frac{2e^2-1}{e^2-1}K_1 - 2eK_2\\
I_3 &= \frac{e(8e^2-5)}{3(e^2-1)}K_1 - \frac{8e^2+1}{3}K_2\\
J_0 &= \frac{4e}{3(e^2-1)^2}K_1 - \frac{1}{3(e^2-1)}K_2\\
J_1 &= \frac{e^2+3}{3(e^2-1)^2}K_1 - \frac{e}{3(e^2-1)}K_2
\end{aligned}\right.$$

$$\left.\begin{aligned}
J_2 &= -\frac{2e(e^2-3)}{3(e^2-1)^2}K_1 + \frac{2e^2-3}{3(e^2-1)}K_2 \\
J_3 &= \frac{-8e^4+15e^2-3}{3(e^2-1)^2}K_1 + \frac{e(8e^2-9)}{3(e^2-1)}K_2 \\
J_4 &= \frac{4e(-4e^4+7e^2-2)}{3(e^2-1)^2}K_1 + \frac{16e^4-16e^2-1}{3(e^2-1)}K_2 \\
K_1 &= \int_0^{\pi}(e-\cos\varphi)^{1/2}\,\mathrm{d}\varphi = \frac{2\sqrt{2}}{k}E(k) \\
K_2 &= \int_0^{\pi}(e-\cos\varphi)^{-1/2}\,\mathrm{d}\varphi = \sqrt{2}kK(k).
\end{aligned}\right\} \tag{17}$$

The complete elliptic integrals

$$K(k) = \int_0^{\pi/2}\frac{d\lambda}{\sqrt{(1-k^2\sin^2\lambda)}}$$

$$E(k) = \int_0^{\pi/2}\sqrt{(1-k^2\sin^2\lambda)}\,\mathrm{d}\lambda$$

have the argument

$$k = \sqrt{\left(\frac{2}{e+1}\right)},\quad e = 1 + \frac{(r-\rho)^2+(z-\zeta)^2}{2r\rho}.$$

4. DEFINITION OF THE BODY FORCE DENSITY

By using the fundamental solutions shown in section 3, the present analysis method is reduced to determining the body force densities distributed along the prospective boundary of a notch or a cylindrical surface imagined in an infinite body. The densities ρ_r, ρ_θ, ρ_z of the body force distributed in the r-, θ-, z-directions are defined in eqns (18)–(20).

(1) In the torsion problem:

(i) along the circumferential groove

$$\rho_\theta = \frac{d}{2\rho}\frac{\mathrm{d}P_\theta}{\rho\,\mathrm{d}\rho\,\mathrm{d}\varphi}; \tag{18a}$$

(ii) along the cylindrical surface

$$\rho_\theta = \frac{\mathrm{d}P_\theta}{\rho\,\mathrm{d}\zeta\,\mathrm{d}\varphi}. \tag{18b}$$

(2) In the tension problem:

(i) along the circumferential groove

$$\rho_r = \frac{\mathrm{d}P_r}{\rho\,\mathrm{d}\varphi\,\mathrm{d}\zeta},\quad \rho_z = \frac{\mathrm{d}P_z}{\rho\,\mathrm{d}\rho\,\mathrm{d}\varphi}; \tag{19a}$$

(ii) along the cylindrical surface

$$\rho_r = \frac{\mathrm{d}P_r}{\rho\,\mathrm{d}\varphi\,\mathrm{d}\zeta},\quad \rho_z = \frac{\mathrm{d}P_z}{\rho\,\mathrm{d}\varphi\,\mathrm{d}\zeta}. \tag{19b}$$

(3) In the bending problem:

(i) along the circumferential groove

$$\left.\begin{aligned} \rho_r \cos\varphi &= \frac{dP_r}{\rho\, d\varphi\, d\zeta}, \quad \rho_\theta \sin\varphi = \frac{dP_\theta}{\rho\, d\varphi\, ds}, \\ \rho_z \cos\varphi &= \frac{d}{2\rho}\frac{dP_z}{\rho\, d\rho\, d\varphi}; \end{aligned}\right\} \tag{20a}$$

(ii) along the cylindrical surface

$$\left.\begin{aligned} \rho_r \cos\varphi &= \frac{dP_r}{\rho\, d\varphi\, d\zeta}, \quad \rho_\theta \sin\varphi = \frac{dP_\theta}{\rho\, d\varphi\, d\zeta}, \\ \rho_z \cos\varphi &= \frac{dP_z}{\rho\, d\varphi\, d\zeta}. \end{aligned}\right\} \tag{20b}$$

In eqns (18)–(20), dP_r, dP_θ, dP_z denote the r-, θ-, z-components, respectively, of the body forces distributed along the infinitesimal area $\rho d\phi ds$ ($ds = \sqrt{((d\rho)^2 + (d\zeta)^2)}$).

The density ρ_θ in he torsion problem (eqn (18a)) is defined considering the torsional stress field

$$\tau_{\theta z}^{\infty} = \tau_0 \frac{2r}{d} \tag{21}$$

where τ_0 is a constant corresponding to the magnitude of the torsional stress. On the other hand, ρ_z in the bending problem (eqn (20a)) is defined considering the bending stress field

$$\sigma_z^{\infty} = \sigma_0 \frac{2r}{d} \cos\theta \tag{22}$$

where σ_0 is a constant corresponding to the magnitude of the bending stress. In the present analysis, the stepped distribution (constant in each interval) of the body force is substituted for the continuously varying distribution. In this procedure, the definition of the body force densities, which make the stepped distribution approximately constant at each interval, should be used. From this viewpoint, the definitions of eqns (18)–(20) are used in the present analysis.

Recently, many researchers have frequently used numerical methods making use of the fundamental solutions similar to those of the body force method; e.g. boundary element method (BEM). However, in the body force method, the unique idea of the body force density enables us to obtain very accurate solutions.

5. PROCEDURE FOR NUMERICAL SOLUTIONS

Figure 6 shows imaginary boundaries where body forces are distributed. Body forces are applied along the part BA′B′ in addition to the part BAB′ which should become a circumferential groove, because it makes the shear stress at B small and consequently the boundary conditions can be satisfied easily. It is difficult to determine in closed form the body force densities satisfying the boundary conditions completely; therefore, the imaginary boundaries are divided and the problem is solved numerically. The boundary of the base of the notch (arc $\widehat{AE}$), the boundary of the flank of the notch (line $\overline{BC}$), and the boundary of the cylindrical surface (line $\overline{BC}$) are divided into n_1, n_2, n_3 intervals, respectively. The boundary length in the z-direction O′C in Fig. 6 is determined from the condition that the calculated results virtually do not change by increasing its length. The minimum value of the length O′C is about two times the cylindrical diameter D. The densities of the body forces, which are assumed to be constant in each interval, are determined from the boundary condition at the midpoint of each interval.

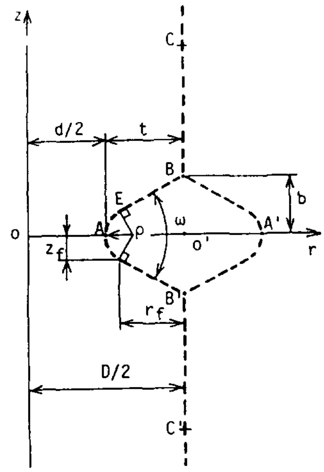

Fig. 6. Imaginary boundaries where body forces are distributed.

By using the fundamental solutions given in Section 4, the influence coefficients $\sigma_i^{\rho rj}$, $\sigma_i^{\rho\theta j}$, $\sigma_i^{\rho zj}$, which mean the stresses induced at the midpoint of the ith interval by the unit body force acting at the jth interval can be written as eqns (23)–(25).

(1) In the torsion problem

$$\left.\begin{aligned} \sigma_i^{\rho\theta j} &= \int_j \sigma^{F_\theta *}|_{F_\theta=1} \frac{2\rho}{d}\,\mathrm{d}\rho \qquad (j = 1 \sim n_1 + n_2) \\ \sigma_i^{\rho\theta j} &= \int_j \sigma^{F_\theta *}|_{F_\theta=1}\,\mathrm{d}\zeta \qquad (j = n_1 + n_2 + 1 \sim n_1 + n_2 + n_3). \end{aligned}\right\} \tag{23}$$

(2) In the tension problem

$$\left.\begin{aligned} &\left.\begin{aligned} \sigma_i^{\rho rj} &= \int_j \sigma^{F_r *}|_{F_r=1}\,\mathrm{d}\zeta \\ \sigma_i^{\rho zj} &= \int_j \sigma^{F_z *}|_{F_z=1}\,\mathrm{d}\rho \end{aligned}\right\} \qquad (j = 1 \sim n_1 + n_2) \\ &\left.\begin{aligned} \sigma^{\rho rj} &= \int_j \sigma^{F_r *}|_{F_r=1}\,\mathrm{d}\zeta \\ \sigma_i^{\rho zj} &= \int_j \sigma^{F_z *}|_{F_z=1}\,\mathrm{d}\zeta \end{aligned}\right\} \qquad (j = n_1 + n_2 + 1 \sim n_1 + n_2 + n_3). \end{aligned}\right\} \tag{24}$$

(3) In the bending problem

$$\left.\begin{aligned} &\left.\begin{aligned} \sigma_i^{\rho rj} &= \int_j \sigma^{F_r \cos\varphi *}|_{F_r=1}\,\mathrm{d}\zeta \\ \sigma_i^{\rho\theta j} &= \int_j \sigma^{F_\theta \sin\varphi *}|_{F_\theta=1}\,\mathrm{d}s \\ \sigma_i^{\rho zj} &= \int_j \sigma^{F_z \cos\varphi *}|_{F_z=1} \frac{2\rho}{d}\,\mathrm{d}\rho \end{aligned}\right\} \qquad (j = 1 \sim n_1 + n_2) \\ &\left.\begin{aligned} \sigma_i^{\rho rj} &= \int_j \sigma^{F_r \cos\varphi *}|_{F_r=1}\,\mathrm{d}\zeta \\ \sigma_i^{\rho\theta j} &= \int_j \sigma^{F_\theta \sin\varphi *}|_{F_\theta=1}\,\mathrm{d}\zeta \\ \sigma_i^{\rho zj} &= \int_j \sigma^{F_z \cos\varphi *}|_{F_z}\,\mathrm{d}\zeta \end{aligned}\right\} \qquad (j = n_1 + n_2 + 1 \sim n_1 + n_2 + n_3) \end{aligned}\right\} \tag{25}$$

where $\int_j$ stands for the integration of jth interval. The integration in eqns (23)–(25) is performed numerically using Gauss's formula. In the case of $i = j$, eqns (23)–(25) become singular and therefore the influence of the body forces must be considered specially [10]. The boundary conditions (B.C.) at the midpoint of the ith interval are expressed by using the influence coefficients as follows.

(1) In the torsion problem:

(i) B.C. of a circumferential groove ($i = 1 \sim n_1 + n_2$)

$$\sum_{j=1}^{n_1+n_2+n_3} \rho_{\theta j}\tau_{n\theta i}^{\rho\theta j} + \tau_0 \frac{2r_i}{d}\sin\psi_i = 0$$

$$\left(\tau_{\theta z}^{\infty} = \tau_0 \frac{2v_i}{d} : \text{torsional stress field due to external torque}\right);$$

(ii) B.C. of a cylindrical surface ($i = n_1 + n_2 + 1 \sim n_1 + n_2 + n_3$) (26)

$$\sum_{j=1}^{n_1+n_2+n_3} \rho_{\theta j}\tau_{r\theta i}^{\rho\theta j} = 0.$$

(2) In the tension problem:

(i) B.C. of a circumferential groove ($i = 1 \sim n_1 + n_2$)

$$\sum_{j=1}^{n_1+n_2+n_3} (\rho_{rj}\sigma_{ni}^{\rho rj} + \rho_{zj}\sigma_{ni}^{\rho zj}) + \sigma_z^{\infty}\cos^2\psi_i = 0$$

$$\sum_{j=1}^{n_1+n_2+n_3} (\rho_{rj}\tau_{nt}^{\rho rj} + \rho_{zj}\tau_{nt}^{\rho zj}) + \sigma_z^{\infty}\sin\psi_i\cos\psi_i = 0$$

(σ_z^{∞}: tensile stress field due to external load); (27)

(ii) B.C. of a cylindrical surface ($i = n_1 + n_2 + 1 \sim n_1 + n_2 + n_3$)

$$\sum_{j=1}^{n_1+n_2+n_3} (\rho_{rj}\sigma_{ri}^{\rho rj} + \rho_{zj}\sigma_{ri}^{\rho zj}) = 0$$

$$\sum_{j=1}^{n_1+n_2+n_3} (\rho_{rj}\tau_{rzi}^{\rho rj} + \rho_{zj}\tau_{rzi}^{\rho zj}) = 0.$$

(3) In the bending problem:

(i) B.C. of a circumferential groove ($i = 1 \sim n_1 + n_2$)

$$\sum_{j=1}^{n_1+n_2+n_3} (\rho_{rj}\sigma_{ni}^{\rho rj} + \rho_{\theta j}\sigma_{ni}^{\rho\theta j} + \rho_{zj}\sigma_{ni}^{\rho zj}) + \sigma_0\frac{2r_i}{d}\cos^2\psi_i = 0$$

$$\sum_{j=1}^{n_1+n_2+n_3} (\sigma_{rj}\tau_{n\theta i}^{\rho rj} + \rho_{\theta j}\tau_{n\theta i}^{\rho\theta j} + \rho_{\theta j}\tau_{n\theta i}^{\rho\theta j}) = 0$$

$$\sum_{j=1}^{n_1+n_2+n_3} (\rho_{rj}\tau_{nti}^{\rho rj} + \rho_{\theta j}\tau_{nti}^{\rho\theta j} + \rho_z\tau_{nti}^{\rho zj}) + \sigma_0\frac{2r_i}{d}\sin\psi_i\cos\psi_i = 0$$

$$\left(\sigma_z^{\infty} = \sigma_0 \frac{2r_i}{d} : \text{bending stress field due to external moment}\right);$$ (28)

(ii) B.C. of a cylindrical surface ($i = n_1 + n_2 + 1 \sim n_1 + n_2 + n_3$)

$$\sum_{d=1}^{n_1+n_2+n_3} (\rho_{rj}\sigma_{ri}^{\rho rj} + \rho_{\theta j}\sigma_{ri}^{\rho\theta j} + \rho_{zj}\sigma_{ri}^{\rho zj}) = 0$$

$$\sum_{j=1}^{n_1+n_2+n_3} (\rho_{rj}\tau_{r\theta i}^{\rho rj} + \rho_{\theta j}\tau_{r\theta i}^{\rho\theta} + \rho_{zj}\tau_{r\theta i}^{\rho zj}) = 0$$

$$\sum (\rho_{rj}\tau_{rzi}^{\rho rj} + \rho_{\theta i}\tau_{rzi}^{\rho\theta j} + \rho_{zj}\tau_{rzi}^{\rho zj}) = 0$$

where r_i is the r-coordinate at the midpoint of the ith interval and ψ_i is the angle between the r-axis and the normal direction of the surface at the same point.

The body force densities are determined by solving n_t, $2n_t$, $3n_t$ linear simultaneous equations in the torsion, tension and bending problem, respectively ($n_t = n_1 + n_2 + n_3$). Once the body force densities are determined, the stresses at an arbitrary point can be easily calculated by using the body force densities and the influence coefficients.

Since the error due to the finiteness of the division number n_t is nearly proportional to $1/n_t$ [9, 10], the value of the stress concentration factor corresponding to $n_t \to \infty$ is obtained by extrapolation of the two values of K_t corresponding to the two values of n_t. Poisson's ratio is assumed to be 0.3.

6. RESULTS AND DISCUSSION

In the following discussion, we use the stress concentration factors (SCFs) based on the net cross-sectional area. They are expressed as follows.

(1) In the torsion problem:

$$K_t = \frac{\tau_{\max}}{\tau_n}, \quad \tau_n = \frac{16T}{\pi d^3} \tag{29}$$

where T is the magnitude of external torque.

(2) In the tension problem:

$$K_t = \frac{\sigma_{\max}}{\sigma_n}, \quad \sigma_n = \frac{4P}{\pi d^2} \tag{30}$$

where P is the magnitude of external load.

(3) In the bending problem:

$$K_t = \frac{\sigma_{\max}}{\sigma_n}, \quad \sigma_n = \frac{32M}{\pi d^3} \tag{31}$$

where M is the magnitude of external moment. Here $\sigma_{\max}$ (or $\tau_{\max}$) is the maximum stress at the root of a notch and σ_{net} (or τ_{net}) is the nominal stress for the minimum diameter d.

6.1 *SCF of a semicircular notch*

There are many reports concerning the problem of a semicircular notch. In particular, Hasegawa has recently obtained accurate solutions in the torsion and tension problems [15, 16]. Therefore, by comparing them with the present results, the accuracy of the present analysis can be estimated.

In Table 1, SCFs of a semicircular notch under torsion, tension and bending are shown. The results obtained by Hasegawa [15, 16] are in close agreement with the present results. The results in Table 1 are plotted in Figs. 7–9.

In Figs. 7–9, the ordinate represents the value of SCFs, and the abscissa represents the

$2\rho/D$	Torsion	Tension	Bending
0.02	1.9087	2.976	2.877
0.03	1.8682	2.928	2.790
0.05	1.7945(1.7946)	2.832(2.824)	2.632
0.1	1.6438(1.6439)	2.601(2.593)	2.307
0.2	1.4353(1.4354)	2.196(2.191)	1.858
0.3	1.3011(1.3012)	1.869(1.871)	1.575
0.4	1.2110(1.2110)	1.610(1.608)	1.390
0.5	1.1481(1.1480)	1.412(1.411)	1.269
0.6	1.1023(1.1023)	1.270(1.270)	1.183
0.7	1.0676(1.0679)	1.172(1.172)	1.120
0.8	1.0403(1.0424)	1.103(1.101)	1.072
0.9	1.0183	1.048(1.046)	1.032

( ) : Hasegawa[15,16]

Table 1. SCFs of a semicircular notch

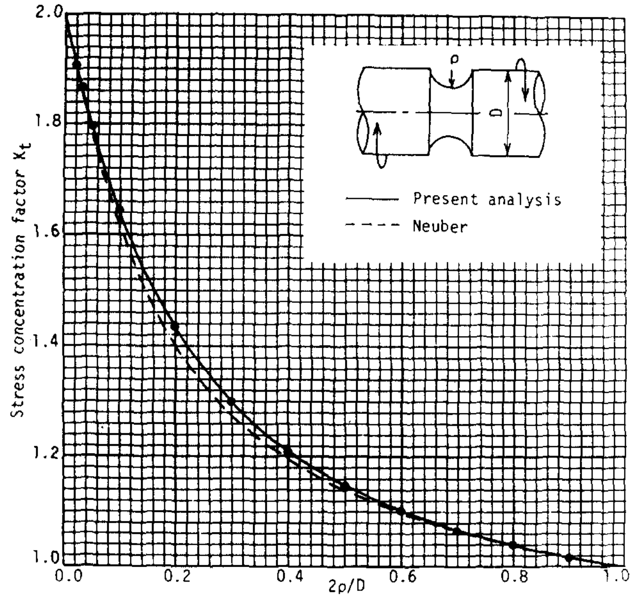

Fig. 7. SCF of a semicircular notch under torsion.

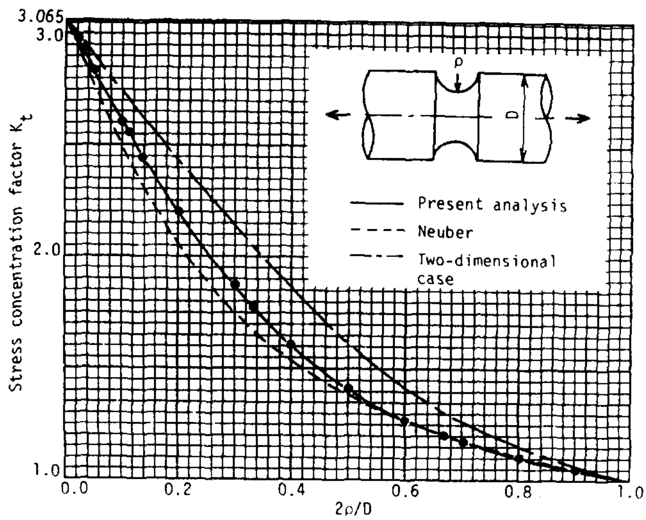

Fig. 8. SCF of a semicircular notch under tension.

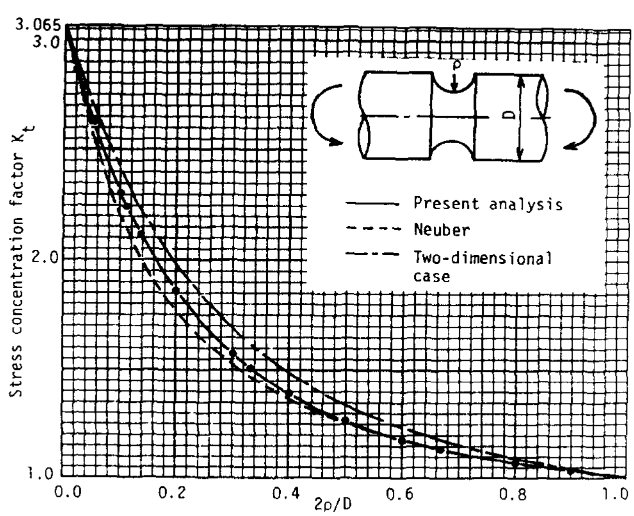

Fig. 9. SCF of a semicircular notch under bending.

2t/D	2ρ/D=0.02			2ρ/D=0.03			2ρ/D=0.05			2ρ/D=0.1		
	K_{tV}	K_{tE}	K_{tN}	K_{tV}	K_{tE}	K_{tN}	K_{tV}	K_{tE}	K_{tN}	K_{tV}	K_{tE}	K_{tN}
0.02	1.91	1.909	1.91	1.720	1.734	1.74	1.538	1.559	1.57	1.361	1.384	1.39
0.05	2.35	2.309	2.28	2.072	2.052	2.03	1.793	1.795	1.78	1.520	1.537	1.53
0.1	2.70	2.619	2.54	2.350	2.294	2.23	1.996	1.969	1.92	1.642	1.644	1.61
0.2	2.91	2.809	2.68	2.517	2.435	2.33	2.115	2.062	1.98	1.711	1.691	1.64
0.3	2.89	2.785	2.65	2.491	2.407	2.30	2.093	2.032	1.95	1.690	1.661	1.61
0.4	2.77	2.671	2.56	2.394	2.311	2.22	2.015	1.954	1.89	1.633	1.602	1.56
0.5	2.60	2.511	2.43	2.258	2.179	2.11	1.909	1.851	1.80	1.559	1.530	1.50
0.6	2.41	2.321	2.26	2.098	2.025	1.98	1.784	1.733	1.70	1.474	1.450	1.43
0.7	2.19	2.103	2.07	1.912	1.848	1.82	1.640	1.599	1.58	1.379	1.360	1.35
0.8	1.91	1.846	1.82	1.691	1.643	1.62	1.474	1.446	1.43	1.272	1.261	1.25
0.9	1.56	1.523	1.51	1.412	1.388	1.38	1.272	1.260	1.25	1.148	1.145	1.14

2t/D	2ρ/D=0.2			2ρ/D=0.5			2ρ/D=1.0		
	K_{tV}	K_{tE}	K_{tN}	K_{tV}	K_{tE}	K_{tN}	K_{tV}	K_{tE}	K_{tN}
0.02	1.241	1.260	1.27	1.137	1.152	1.16	1.088	1.098	1.10
0.05	1.336	1.356	1.35	1.183	1.199	1.19	1.111	1.123	1.12
0.1	1.404	1.418	1.39	1.209	1.224	1.21	1.122	1.133	1.12
0.2	1.435	1.435	1.40	1.213	1.221	1.20	1.118	1.125	1.11
0.3	1.415	1.408	1.37	1.197	1.200	1.18	1.106	1.110	1.10
0.4	1.375	1.365	1.34	1.174	1.175	1.16	1.093	1.095	1.09
0.5	1.326	1.316	1.30	1.148	1.148	1.14	1.078	1.079	1.08
0.6	1.272	1.264	1.25	1.121	1.121	1.12	1.063	1.064	1.06
0.7	1.212	1.207	1.20	1.093	1.092	1.09	1.048	1.048	1.05
0.8	1.148	1.146	1.14	1.063	1.063	1.06	1.033	1.033	1.03
0.9	1.078	1.078	1.08	1.032	1.032	1.03	1.017	1.017	1.02

Table 2. SCFs of a 60° V-shaped notch under torsion

K_{tV}: SCF of a 60° V-shaped notch
K_{tE}: SCF of a semielliptical notch
K_{tN}: SCF of Neuber's rule

2t/D	2ρ/D=0.03			2ρ/D=0.05			2ρ/D=0.1		
	K_{tV}	K_{tE}	K_{tN}	K_{tV}	K_{tE}	K_{tN}	K_{tV}	K_{tE}	K_{tN}
0.02	2.571	2.598	2.55	2.193	2.221	2.19	1.816	1.847	1.83
0.05	3.424	3.411	3.27	2.824	2.832	2.74	2.232	2.257	2.20
0.1	4.181	4.122	3.87	3.387	3.359	3.18	2.596	2.601	2.48
0.2	4.790	4.678	4.32	3.827	3.755	3.49	2.865	2.836	2.64
0.3	4.883	4.741	4.38	3.877	3.781	3.51	2.871	2.824	2.63
0.4	4.732	4.571	4.26	3.742	3.633	3.39	2.754	2.697	2.53
0.5	4.423	4.265	4.02	3.495	3.384	3.20	2.566	2.506	2.38
0.6	4.013	3.865	3.70	3.171	3.065	2.94	2.330	2.274	2.19
0.7	3.516	3.381	3.28	2.777	2.689	2.61	2.055	2.010	1.97
0.8	2.910	2.802	2.75	2.314	2.247	2.21	1.742	1.718	1.70
0.9	2.139	2.077	2.06	1.739	1.712	1.71	1.387	1.386	1.39

2t/D	2ρ/D=0.2			2ρ/D=0.5			2ρ/D=1.0		
	K_{tV}	K_{tE}	K_{tN}	K_{tV}	K_{tE}	K_{tN}	K_{tV}	K_{tE}	K_{tN}
0.02	1.555	1.586	1.58	1.331	1.356	1.35	1.221	1.241	1.23
0.05	1.827	1.856	1.81	1.476	1.505	1.46	1.305	1.330	1.29
0.1	2.050	2.071	1.97	1.582	1.609	1.53	1.356	1.382	1.31
0.2	2.196	2.196	2.05	1.624	1.641	1.53	1.356	1.374	1.30
0.3	2.172	2.158	2.01	1.581	1.587	1.50	1.313	1.322	1.27
0.4	2.071	2.048	1.93	1.503	1.504	1.45	1.260	1.263	1.24
0.5	1.928	1.903	1.82	1.414	1.412	1.38	1.209	1.208	1.21
0.6	1.760	1.740	1.70	1.325	1.323	1.32	1.164	1.162	1.17
0.7	1.579	1.567	1.55	1.240	1.240	1.24	1.123	1.122	1.13
0.8	1.389	1.388	1.39	1.161	1.162	1.17	1.084	1.083	1.09
0.9	1.199	1.201	1.21	1.084	1.085	1.09	1.043	1.044	1.04

Table 3. SCFs of a 60° V-shaped notch under tension

K_{tV}: SCF of a 60° V-shaped notch
K_{tE}: SCF of a semielliptical notch
K_{tN}: SCF of Neuber's rule

relative notch radius $2\rho/D$. Neuber's corresponding values are designated by the dashed line. In the tension and bending problem, results of two-dimensional strip problems obtained by Ling [17, 18] and Isida [19, 20] are also designated by the dash-dotted line. As $2c/D \to 0$, the results of the present analysis approach the corresponding two-dimensional values ($K_t = 3.065$ or 2), and as $2c/D \to 1$, they approach the value $K_t = 1$.

6.2 *SCF of a 60° V-shaped notch*

Tables 2–4 show SCFs of a 60° V-shaped notch (K_{tV}) under torsion, tension and bending. In the case of a shallow notch ($t \leqq \rho/2$), K_{tV} means SCF of a circular-arc notch. The values

	$2\rho/D=0.03$			$2\rho/D=0.05$			$2\rho/D=0.1$		
$2t/D$	K_{tV}	K_{tE}	K_{tN}	K_{tV}	K_{tE}	K_{tN}	K_{tV}	K_{tE}	K_{tN}
0.02	2.50	2.511	2.48	2.120	2.147	2.13	1.753	1.785	1.78
0.05	3.19	3.169	3.06	2.629	2.630	2.56	2.078	2.099	2.05
0.1	2.71	3.648	3.45	3.003	2.974	2.83	2.305	2.306	2.21
0.2	3.99	3.893	3.64	3.187	3.124	2.95	2.396	2.375	2.25
0.3	3.91	3.796	3.58	3.111	3.035	2.88	2.325	2.293	2.19
0.4	3.69	3.579	3.42	2.942	2.868	2.75	2.203	2.164	2.09
0.5	3.42	3.308	3.20	2.724	2.656	2.58	2.049	2.017	1.97
0.6	3.10	3.007	2.93	2.480	2.424	2.37	1.884	1.860	1.83
0.7	2.73	2.667	2.61	2.204	2.168	2.12	1.704	1.692	1.67
0.8	2.30	2.27	2.22	1.884	1.87	1.84	1.501	1.499	1.48
0.9	1.77	1.77	1.73	1.502	1.51	1.48	1.269	1.27	1.26

	$2\rho/D=0.2$			$2\rho/D=0.5$			$2\rho/D=1.0$		
$2t/D$	K_{tV}	K_{tE}	K_{tN}	K_{tV}	K_{tE}	K_{tN}	K_{tV}	K_{tE}	K_{tN}
0.02	1.502	1.532	1.53	1.288	1.311	1.31	1.185	1.202	1.19
0.05	1.699	1.728	1.69	1.382	1.407	1.37	1.232	1.250	1.22
0.1	1.827	1.845	1.77	1.428	1.450	1.40	1.246	1.262	1.22
0.2	1.857	1.858	1.77	1.416	1.427	1.38	1.223	1.232	1.21
0.3	1.794	1.786	1.72	1.370	1.375	1.35	1.193	1.198	1.19
0.4	1.703	1.695	1.65	1.318	1.320	1.31	1.165	1.167	1.16
0.5	1.603	1.596	1.57	1.267	1.269	1.26	1.139	1.139	1.14
0.6	1.498	1.494	1.48	1.217	1.218	1.21	1.112	1.112	1.11
0.7	1.388	1.388	1.38	1.165	1.166	1.16	1.085	1.085	1.09
0.8	1.270	1.272	1.26	1.112	1.113	1.11	1.058	1.058	1.06
0.9	1.143	1.14	1.14	1.059	1.058	1.06	1.028	1.028	1.03

Table 4. SCFs of a 60° V-shaped notch under bending

[K_{tV}: SCF of a 60° V-shaped notch
K_{tE}: SCF of a semielliptical notch
K_{tN}: SCF of Neuber's rule]

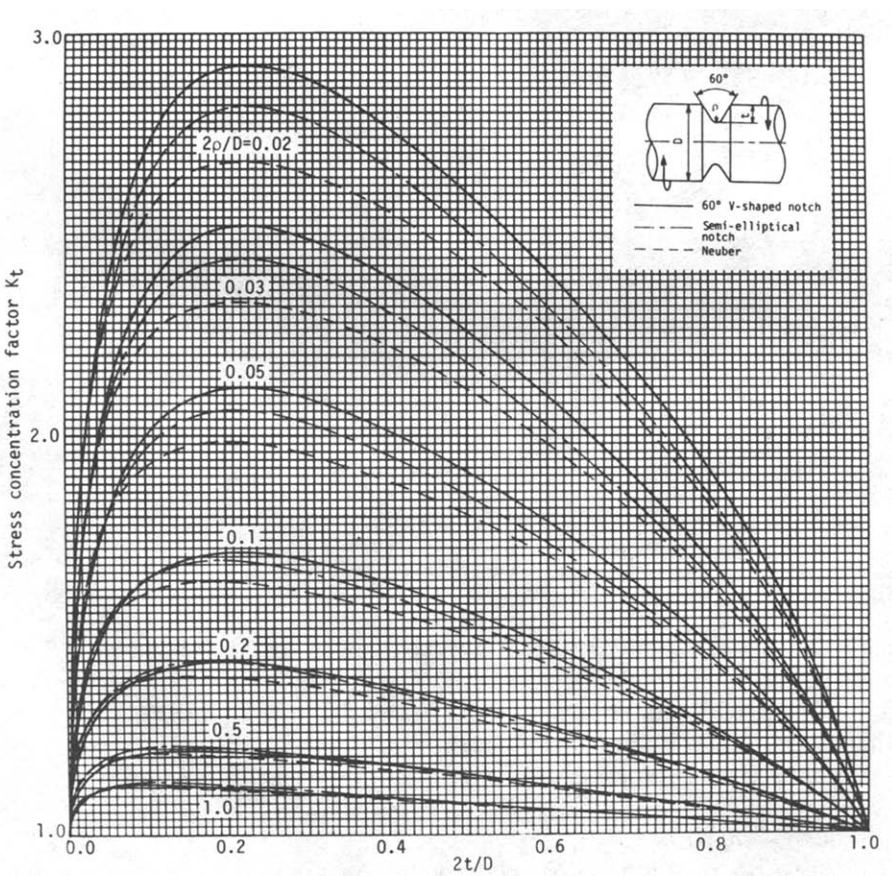

Fig. 10. SCF of a 60° V-shaped notch under torsion.

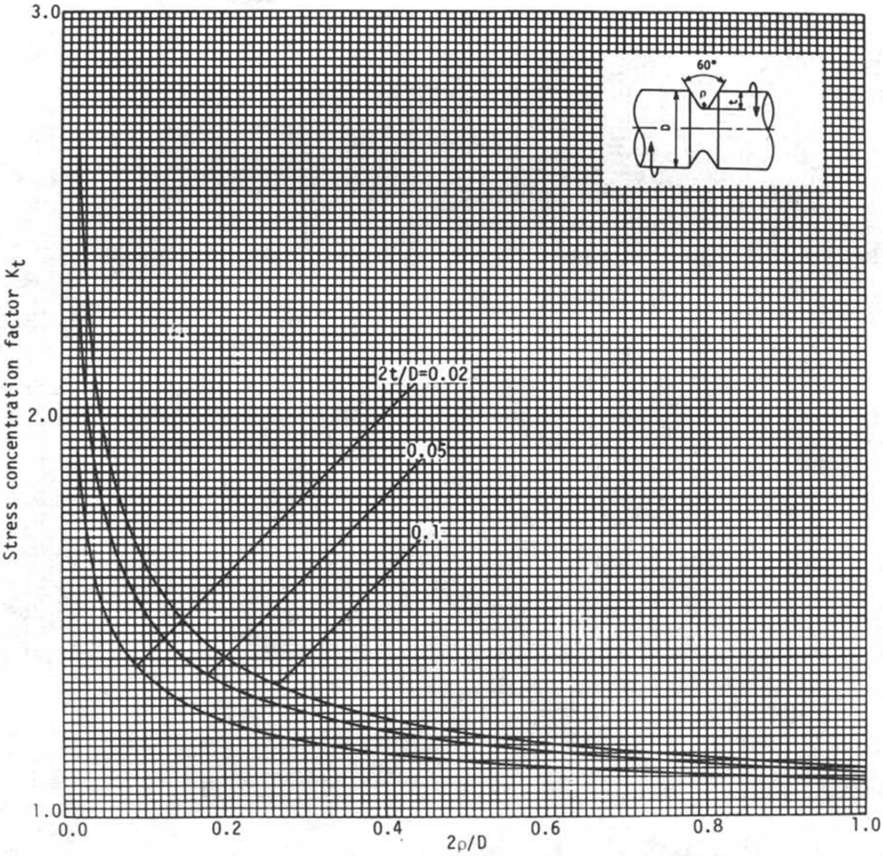

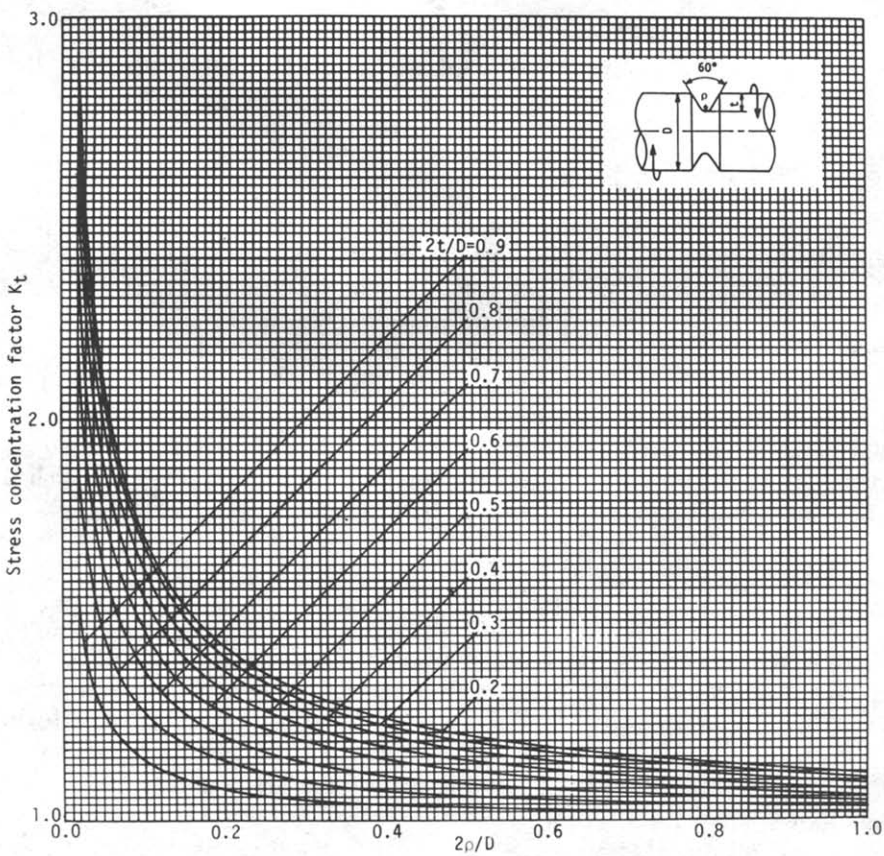

Fig. 11(a) and (b). SCF of a 60° V-shaped notch under torsior

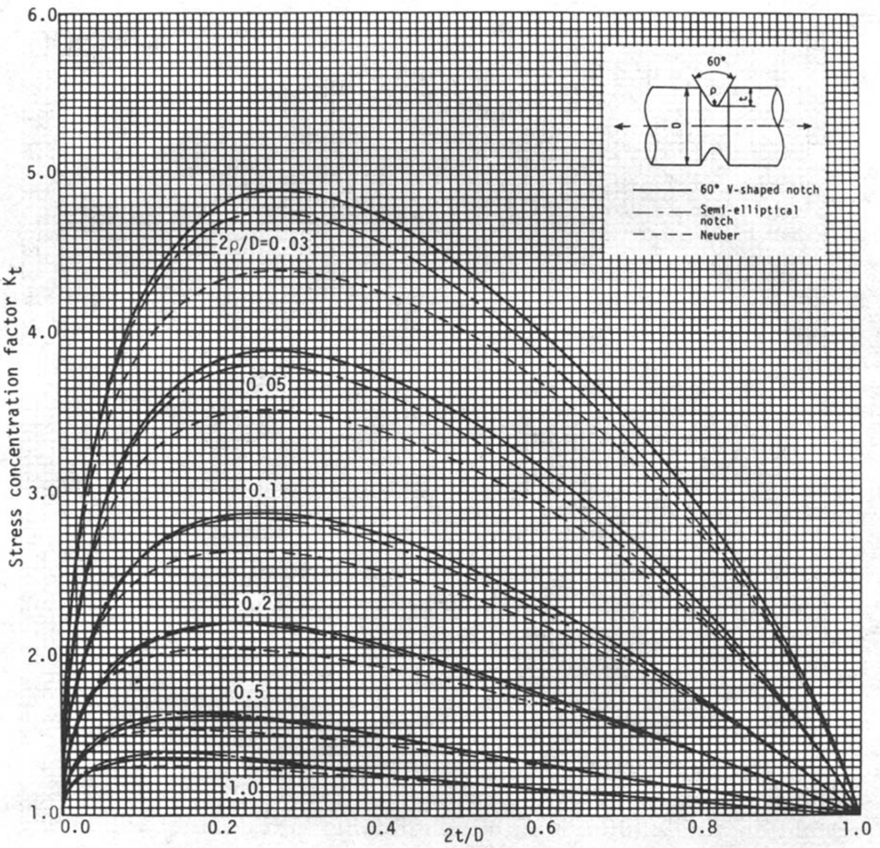

Fig. 12. SCF of a 60° V-shaped notch under tension.

of a semielliptical notch (K_{tE}), which are similarly calculated by the present method, and the Neuber's values (K_{tN}, eqn (1)) are also shown to be compared with the values of a 60° V-shaped notch. The results in Tables 2–4 are plotted in Figs. 10–15 so as to be useful for further design or research.

In Figs. 10, 12 and 14, the ordinate represents the values of SCFs, and the abscissa represents the relative notch depth $2t/D$. Comparisons between the values of a 60° V-shaped notch and the semielliptical notch indicate that the difference between them ($K_{tV} > K_{tE}$) becomes larger as the notch radius becomes smaller. The reason is that the difference between the 60° V-shape and the semiellipse becomes larger as the notch radius becomes smaller.

By systematic calculation shown in Tables 2–4, we conclude that Neuber's rule (eqn (1)) underestimates SCFs of the 60° V-shaped notch by about 10% for a wide range of notch depths in torsion, tension and bending problems.

The charts of SCF are also shown in different ways from Figs. 10, 12 and 14. In Figs. 11, 13 and 15, the abscissa represents the relative notch radius $2\rho/D$. Using these charts (Figs. 10–15), SCF K_{tV} not calculated in this paper will be estimated.

7. CONCLUSION

Since there were no exact solutions for the problem of a cylindrical bar with a circumferential groove under torsion, tension and bending, the approximate stress concentration factors by Neuber's rule have been used for a long time. It has been supposed that the error of Neuber's values is not so large; however, there have been few discussions about the accuracy. In the present study, the problem is analyzed by the body force method. The conclusions are summarized as follows:

(1) Stress concentration factors of a cylindrical bar with a 60° V-shaped circumferential groove under torsion, tension and bending are systematically calculated for various geometrical

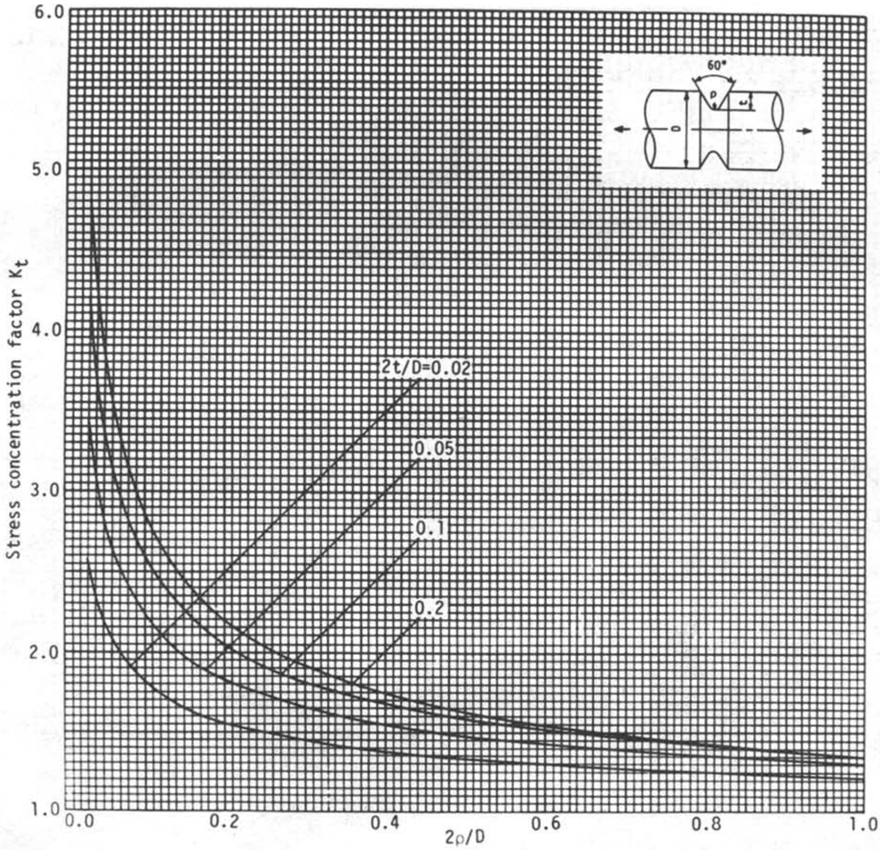

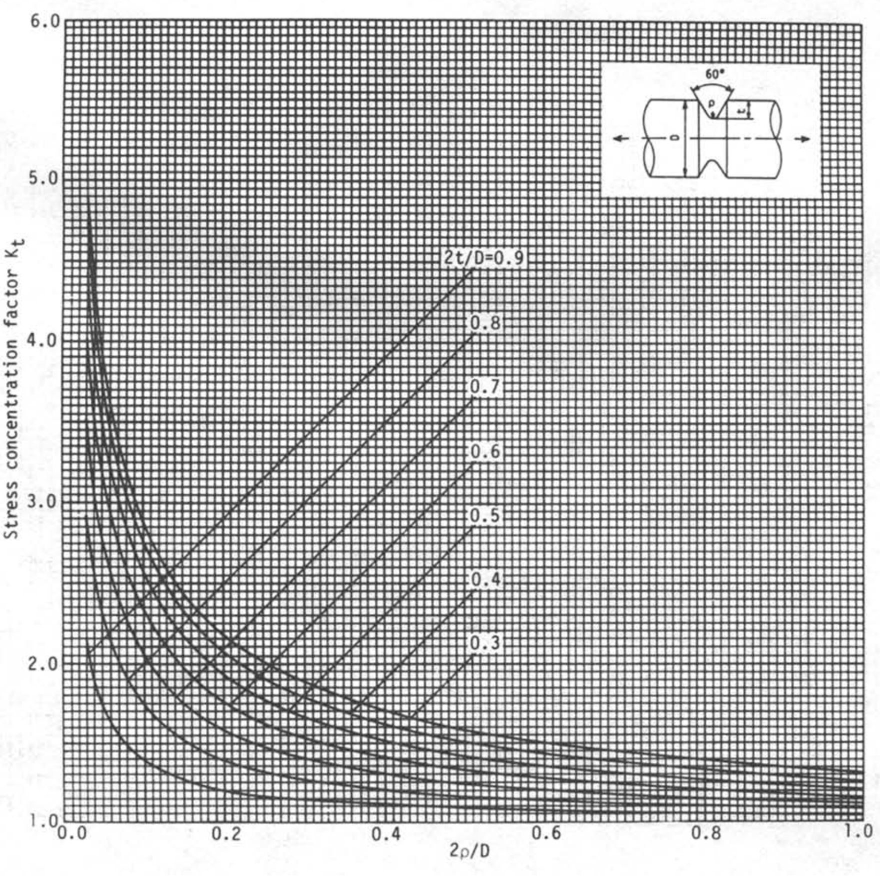

Fig. 13(a) and (b). SCF of a 60° V-shaped notch under tension.

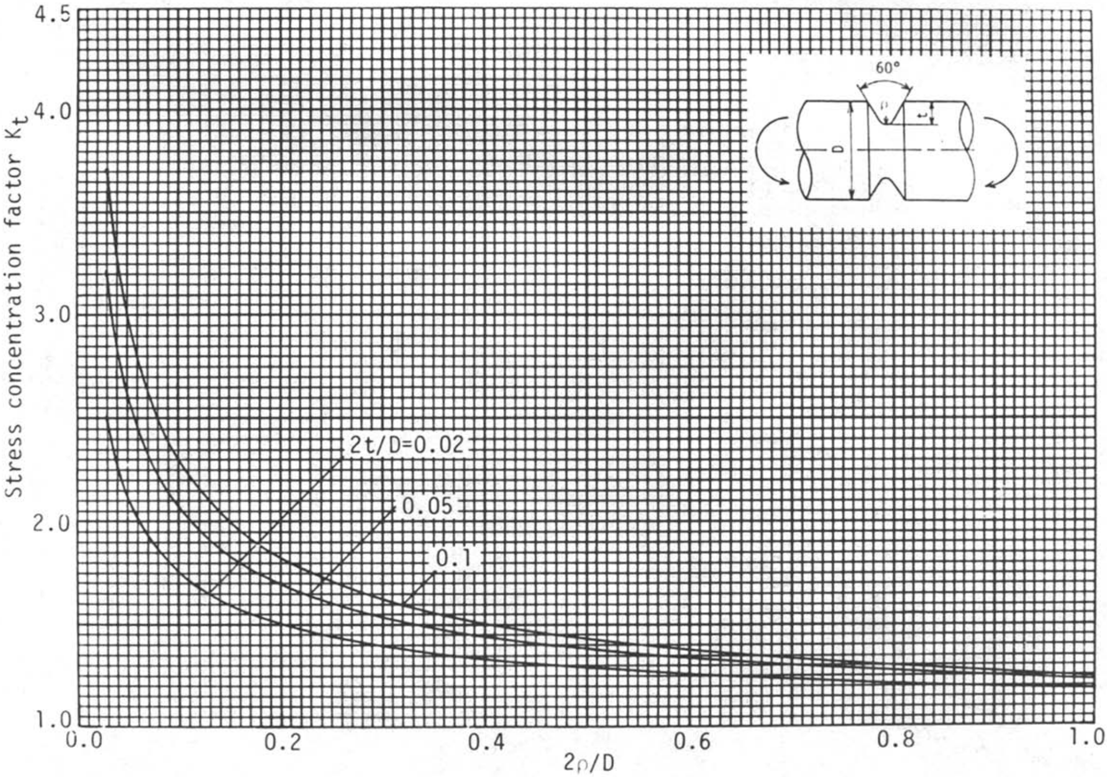

Fig. 14. SCF of a 60° V-shaped notch under bending.

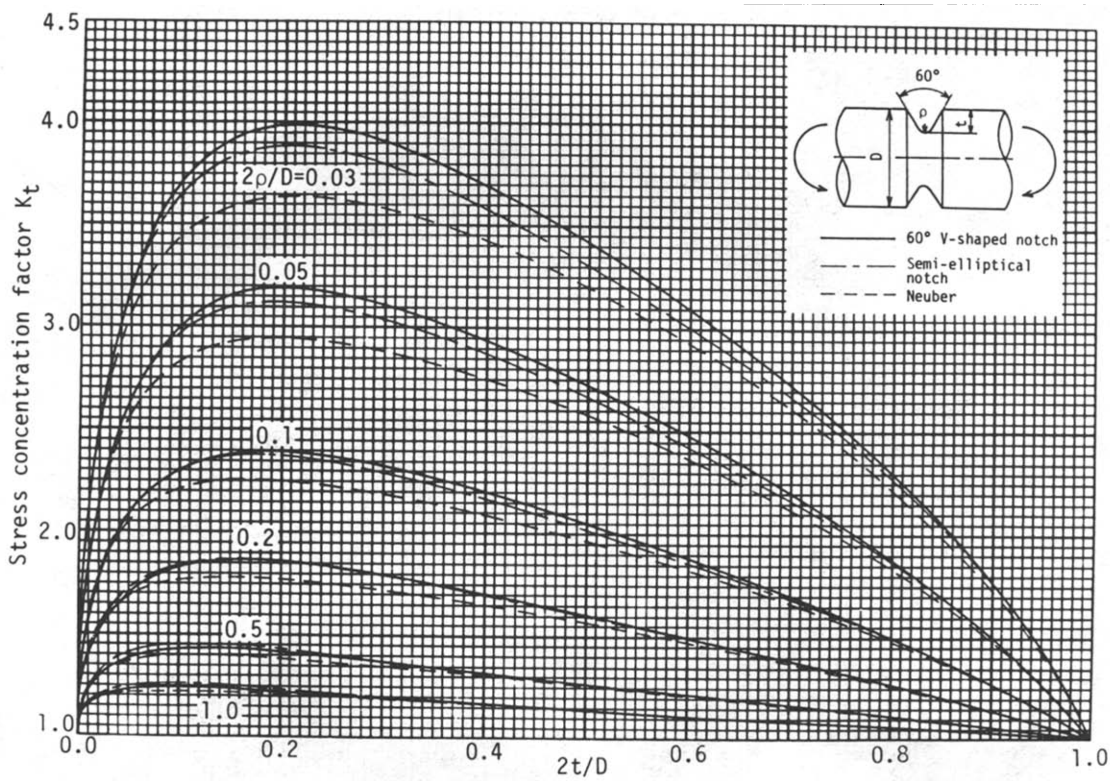

Fig. 15(a). SCF of a 60° V-shaped notch under bending.

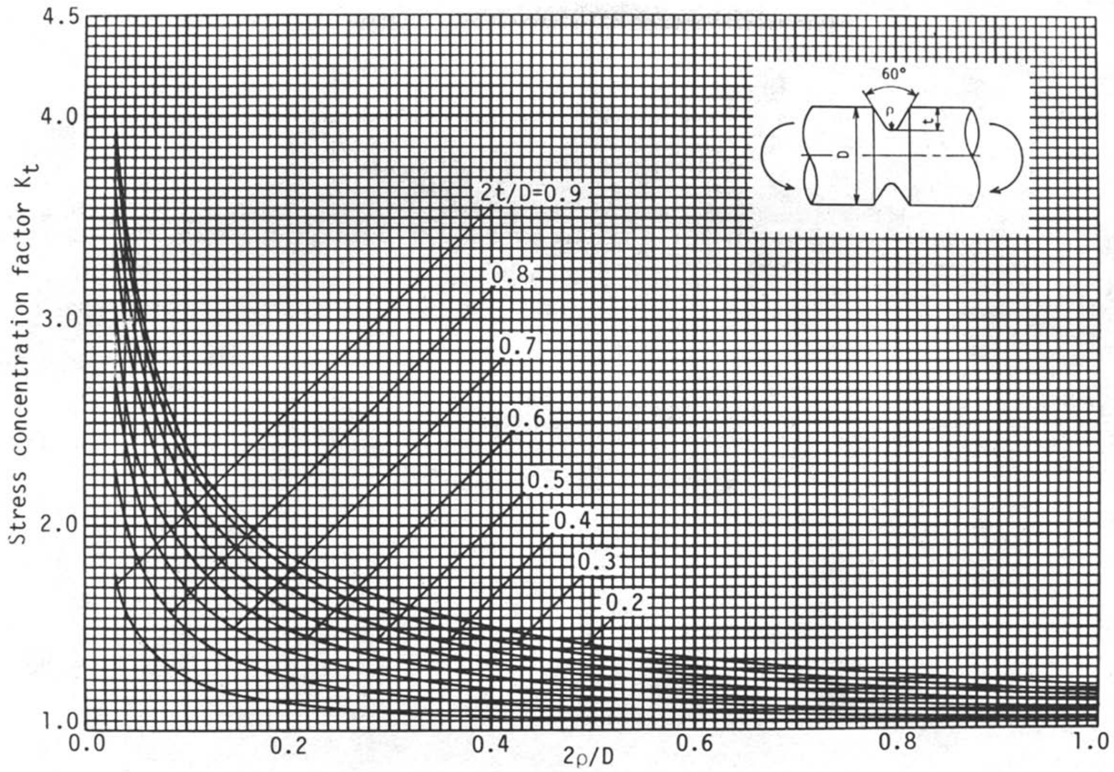

Fig. 15. (b). SCF of a 60° V-shaped notch under bending, cont.

conditions. It is found that Neuber's rule has a non-conservative error of about 10% for a wide range of notch depths in the torsion, tension and bending problems.

(2) The stress concentration factors are illustrated in charts (Figs. 10–15) so as to be used easily in design or research.

(3) The present results of a semicircular notch in torsion and tension problems are in close agreement with Hasegawa's solutions (Table 1).

(4) The fundamental solutions and the procedure for numerical solutions given in the present paper are utilized for the analysis of the other problems of an axisymmetric body under torsion, tension or bending.

REFERENCES

[1] H. Neuber, *Kerbspannungslehre*. Springer, Berlin (1958).
[2] R. E. Peterson, *Stress Concentration Design Factors*. Wiley, New York (1962).
[3] M. Nisida, *Stress Concentration* (in Japanese). Morikitashuppan, Tokyo (1962).
[4] K. R. Rushton, Stress concentration arising in the torsion of grooved shafts. *Int. J. Mech. Sci.* **9**, 697–705 (1967).
[5] M. Kikukawa and Y. Sato, Stress concentration in notched bars under tension or bending (2nd Report, U-grooved shafts). *Trans. Japan Soc. Mech. Engrs. (JSME)* **38**, 1673–1680 (1972).
[6] M. Kikukawa and Y. Sato, Stress concentration in notched bars under tension or bending (3rd Report, V-notched strip, V-grooved shafts and shouldered shafts). *Trans. Japan Soc. Mech. Engrs. (JSME)* **38**, 1681–3709 (1972).
[7] H. Miyamoto, Calculation of stress concentration factors by finite element method. *J. Japan Soc. Precision Engrs* **35**, 609–623 (1969).
[8] Y. Sato, M. Kikukawa and T. Matsui, Stress concentration in notched bars under tension or bending (4th Report, Finite element analysis of semicircular shafts). *Trans. Japan Soc. Mech. Engrs (JSME)* **42**, 3701–3709 (1976).
[9] H. Nisitani, The two-dimensional stress problem solved using an electric digital computer. *J. Japan Soc. Mech. Engrs (JSME)* **70**, 627–632 (1967). [*Bull. Japan Soc. Mech. Engrs (JSME)* **11**, 14–23 (1968).]
[10] H. Nisitani, Solution of notch problems by body force method. *Stress Analysis of Notched Problems* (Edited by G. C. Sih), pp. 1–68. Noordhoff, Leyden (1978).
[11] H. Nisitani, Interference effect among cracks or notches in two-dimensional problems, *Proc. Int. Conf. on Fracture Mechanics and Technology* (Edited by G.C. Sih and C. L. Chow), pp. 1127–1142. Sijthoff and Noordhoff (1977).
[12] H. Nisitani and Y. Murakami, Stress intensity factors of an elliptical crack or a semi-elliptical crack subjected to tension. *Int. J. Fracture* **10**, 353–368 (1974).
[13] M. Isida and H. Noguchi, Tension of plates containing an embedded elliptical crack. *Trans. Japan Soc. Mech. Engrs (JSME)* **48**, 888–898 (1982).

[14] Y. Murakami and S. Nemat-Nasser, Growth and stability of interacting surface flows of arbitrary shape. *Engng Fract. Mech.* **17-3,** 193–210 (1983).
[15] H. Hasegawa, On the stress concentration problem of a shaft with a semicircular groove under tension. *Trans. Jspan Soc. Mech. Engrs (JSME)* **46,** 805–814 (1970).
[16] H. Hasegawa and Y. Kuriyama, Torsion of an elastic solid cylinder with one or two semicircular grooves. *Trans. Japan Soc. Mech. Engrs (JSME)* **49,** 838–846 (1983).
[17] C. B. Ling, Stresses in a notched strip under tension. *J. Appl. Mech.* **14-4,** 275–280 (1947).
[18] C. B. Ling, Stresses in a notched strip. *J. Appl. Mech* **19-2,** 141–146 (1952).
[19] M. Isida, On the tension of the strip with semicircular notches. *Trans. Japan Soc. Mech. Engrs* **19-87,** 5–10 (1953).
[20] M. Isida, On the bending of a strip with semicircular notches. *Trans. Japan Soc. Mech. Engrs (JSME),* **19-87,** 94–99 (1953).
[21] Y. Murakami, N. Noda and H. Nisitani, Application of body force method to the analysis of stress concentration of an axisymmetric body under bending (First Report, Basic theory and application to several simple problems. *Trans. Japan Soc. Mech. Engrs (JSME)* **48,** 301–311 (1982).